Illusions and cloaks for surface waves.

McManus, TM; Valiente-Kroon, JA; Horsley, SA; Hao, Y

For additional information about this publication click this link.
http://qmro.qmul.ac.uk/xmlui/handle/123456789/13154

Information about this research object was correct at the time of download; we occasionally make corrections to records, please therefore check the published record when citing. For more information contact scholarlycommunications@qmul.ac.uk

Illusions and Cloaks for Surface Waves

T. M. McManus[1], J. A. Valiente-Kroon[2], S. A. R. Horsley[3] & Y. Hao[1]

[1]School of Electronic Engineering and Computer Science, Queen Mary University of London, E1 4NS, England, UK, [2]School of Mathematical Sciences, Queen Mary University of London, E1 4NS, England, UK, [3]Department of Physics and Astronomy, University of Exeter, EX4 4QL, England, UK.

Ever since the inception of Transformation Optics (TO), new and exciting ideas have been proposed in the field of electromagnetics and the theory has been modified to work in such fields as acoustics and thermodynamics. The most well-known application of this theory is to cloaking, but another equally intriguing application of TO is the idea of an illusion device. Here, we propose a general method to transform electromagnetic waves between two arbitrary surfaces. This allows a flat surface to reproduce the scattering behaviour of a curved surface and vice versa, thereby giving rise to perfect optical illusion and cloaking devices, respectively. The performance of the proposed devices is simulated using thin effective media with engineered material properties. The scattering of the curved surface is shown to be reproduced by its flat analogue (for illusions) and vice versa for cloaks.

To date, almost all examples of TO[1–6] devices such as cloaking[7–12] and optical illusion[13–16] were concerned primarily with three-dimensional free space waves and although those devices were successfully modelled, their practical applications have been hampered by the fundamental limits of their required material parameters which were lossy, dispersive and narrowband. In an attempt to reduce the complexity of the required materials of the devices, we will investigate TO for two-dimensional surfaces, which do not rely upon any symmetry.

This Letter presents a general method to achieve illusion devices for surface waves, with the aim of utilising a flat, anisotropically loaded medium to perfectly recreate the total scattering characteristics of an arbitrarily, curved surface for all angles of incidence. For the cloaking device[17], a similar derivation to that of the illusion device is employed, and an anisotropically loaded, curved deformation is shown to behave as if it were a flat surface for all angles of incidence. The proposed illusion and cloaking devices, serve as proofs-of-concepts that can be adapted to other waves, e.g. acoustic.

The underlying theory of the proposed illusion device is as follows. Starting with a flat surface, upon which electromagnetic waves are confined (e.g. a thin waveguide) we add an anisotropic layer, which modifies the effective space through which the waves propagate. If done properly, this material distribution[18–21] will emulate the behaviour of a surface wave along a curved surface, thus giving rise to an illusion device. The proposed method is derived in the approximation of Geometrical Optics (GO). We write the electric field as an amplitude times a phase, $\mathbf{E} = \boldsymbol{a}e^{iS}$, and assume that the phase of the wave varies much more quickly than the amplitude or the properties of the medium. Maxwell's equations are then recast as

$$\nabla S \cdot \varepsilon \cdot \boldsymbol{a} = 0, \tag{1a}$$

$$\frac{1}{\omega}(\nabla S \times \boldsymbol{a})e^{iS} = \boldsymbol{B}, \tag{1b}$$

$$\nabla S \times \boldsymbol{\mu}^{-1} \cdot (\nabla S \times \boldsymbol{a}) + \omega^2 \varepsilon \cdot \boldsymbol{a} = 0. \tag{1c}$$

Assuming that the medium is in an electrically thin waveguide, the fundamental mode is uniform for the cavity and that $\mathbf{E}$ is always normal to the top and bottom of the waveguide, we have $\varepsilon_{zi} = \delta_{zz}$ and $\boldsymbol{a} = a\hat{\boldsymbol{z}}$. Then ∇S lies exclusively in the x-y plane, meaning that equation (1c) can be recast as

$$\frac{1}{\det(\tilde{\boldsymbol{\mu}})}\left[\mu_{xx}\left(\frac{\partial S}{\partial x}\right)^2 + 2\left(\frac{\partial S}{\partial x}\right)\left(\frac{\partial S}{\partial y}\right)\mu_{xy} + \mu_{yy}\left(\frac{\partial S}{\partial y}\right)^2\right] = \omega^2 \tag{2}$$
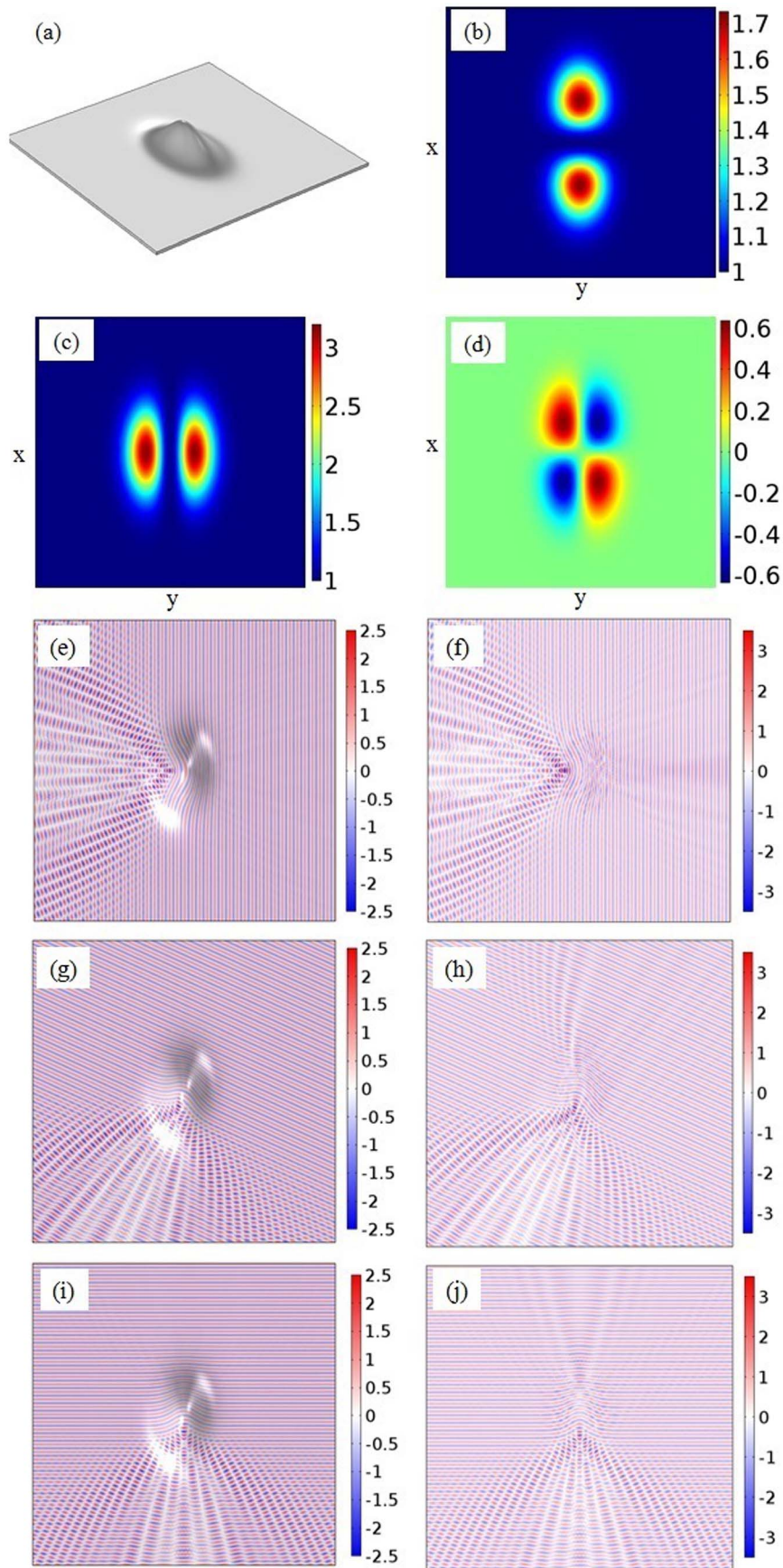
where

1

Figure 1 | Single deformation illusion device. (a) Isometric view of S_1. (b) ε,μ_{xx}. (c) ε,μ_{yy}. (d) ε,μ_{xy}. Plane wave propagating (E_z) from right to left ($\theta_i = 0$), for curved isotropic medium (e) and flat anisotropic medium (f). Plane wave propagating (E_z) at $\theta_i = \dfrac{\pi}{3}$ for curved isotropic medium (g) and flat anisotropic medium (h). Plane wave propagating (E_z) at $\theta_i = \dfrac{\pi}{2}$ for curved isotropic medium (i) and flat anisotropic medium (j).
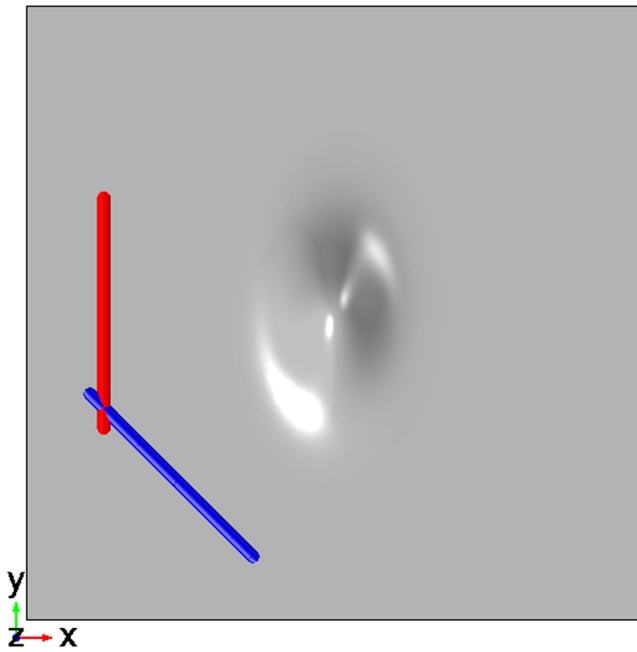
Figure 2 | Probe line locations for illusion device validation.

Figure 3 | Quantitative validation of proposed illusion device. (a) $\theta_i = 0$ (b) $\theta_i = \frac{\pi}{4}$.

$$\boldsymbol{\mu} = \begin{pmatrix} \tilde{\boldsymbol{\mu}} & 0 \\ 0 & 1 \end{pmatrix}, \tag{3}$$

as is noted in[22]. In what follows it is assumed that the surface to be simulated is of the form $z = \sigma(x,y)$. Now, in order to relate the properties of $\boldsymbol{\mu}$ to the geometry of an arbitrary surface consider the eikonal equation in a general 2D coordinate system

$$\tilde{g}^{ln} \frac{\partial s}{\partial x^n} \frac{\partial s}{\partial x^l} = \omega^2. \tag{4}$$

Comparing equations (2) and (4) we find the following relationship between the material properties in the waveguide and an equivalent 2D metric tensor

$$\frac{\tilde{\boldsymbol{\mu}}}{\det(\tilde{\boldsymbol{\mu}})} = \tilde{\boldsymbol{g}}^{-1}. \tag{5}$$

Taking the determinant of both sides and using the fact that $\boldsymbol{\mu}$ is a 2×2 matrix one finds that

$$\frac{1}{\det(\tilde{\boldsymbol{\mu}})} = \frac{1}{\det(\tilde{\boldsymbol{g}})} \tag{6}$$

and the following equivalence can be established

$$\begin{pmatrix} \mu_{xx} & \mu_{xy} \\ \mu_{xy} & \mu_{yy} \end{pmatrix} = \begin{pmatrix} 1 + \left(\frac{\partial \sigma}{\partial y}\right)^2 & -\left(\frac{\partial \sigma}{\partial x}\right)\left(\frac{\partial \sigma}{\partial y}\right) \\ -\left(\frac{\partial \sigma}{\partial x}\right)\left(\frac{\partial \sigma}{\partial y}\right) & 1 + \left(\frac{\partial \sigma}{\partial x}\right)^2 \end{pmatrix}. \tag{7}$$

Having constructed a relationship between the constitutive parameters of a flat surface, and an equivalent deformed surface, we proceed to test this equivalence. The first surface, S_1, is simply a skewed Gaussian deformation (Fig. 1a) that has a height profile describe by $z_1 = e^{-(3x^2 + y^2)}$ and will act as the archetypal, rotationally asymmetric surface in this study. This surface deformation is approximately $1\lambda_0 \times 20\lambda_0 \times 5\lambda_0$ in the x, y and z-directions, respectively. The method of excitation employed herein was established in[12,23,24] and is effectively a plane wave with the E-field polarized in the Z-direction with an amplitude of 1 V/m. Applying the equivalence given in equation (7), we arrive at the required permittivity and
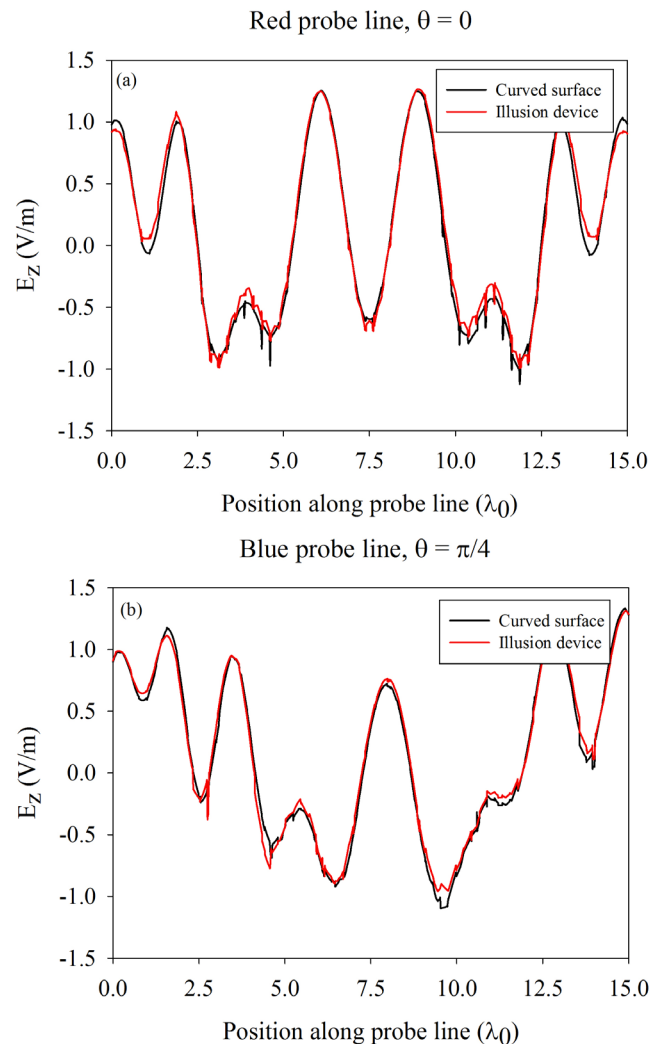
permeability tensors (Fig. 1b–d) that will make a flat metallic surface coated with thin anisotropic materials appear (electrically speaking) to surface waves, as if it were in fact a curved isotropic surface described by z_1.

In Fig. 1e–j, we observe the agreement between surface wave scattering (SWS) from the curved and flat surfaces (Animation 1 and Animation 2, respectively). As was mentioned earlier, though more emphasis is placed on the forward-SWS behavior with regards to illusion devices, the near-perfect reproduction of backward-SWS should not be overlooked if for no other reason, than as a performance metric to gauge the fidelity of the proposed technique. Here it is also important to point out that for both illusion and cloaking devices the primary goal is to reproduce phase fronts that occur a number of wavelengths away from the surface deformation, and not necessarily the amplitude. In the case of the illusion device, we see that the range of the amplitude of E_z is not the same for both the curved surface and its flattened analogue, though they are of the same order of magnitude, and in turn not inherently cause for concern. The reason for this difference is that in the case of the curved surface, there is effectively a degree of smooth-body diffraction occurring as the surface wave traverses the deformation which then leads to an interference pattern in the "shadow region" of the deformation. This same effect cannot be recreated by the flattened illusion device because it is borne out of GO which by definition does not take into account any form of diffraction. In order to truly appreciate the fidelity of the
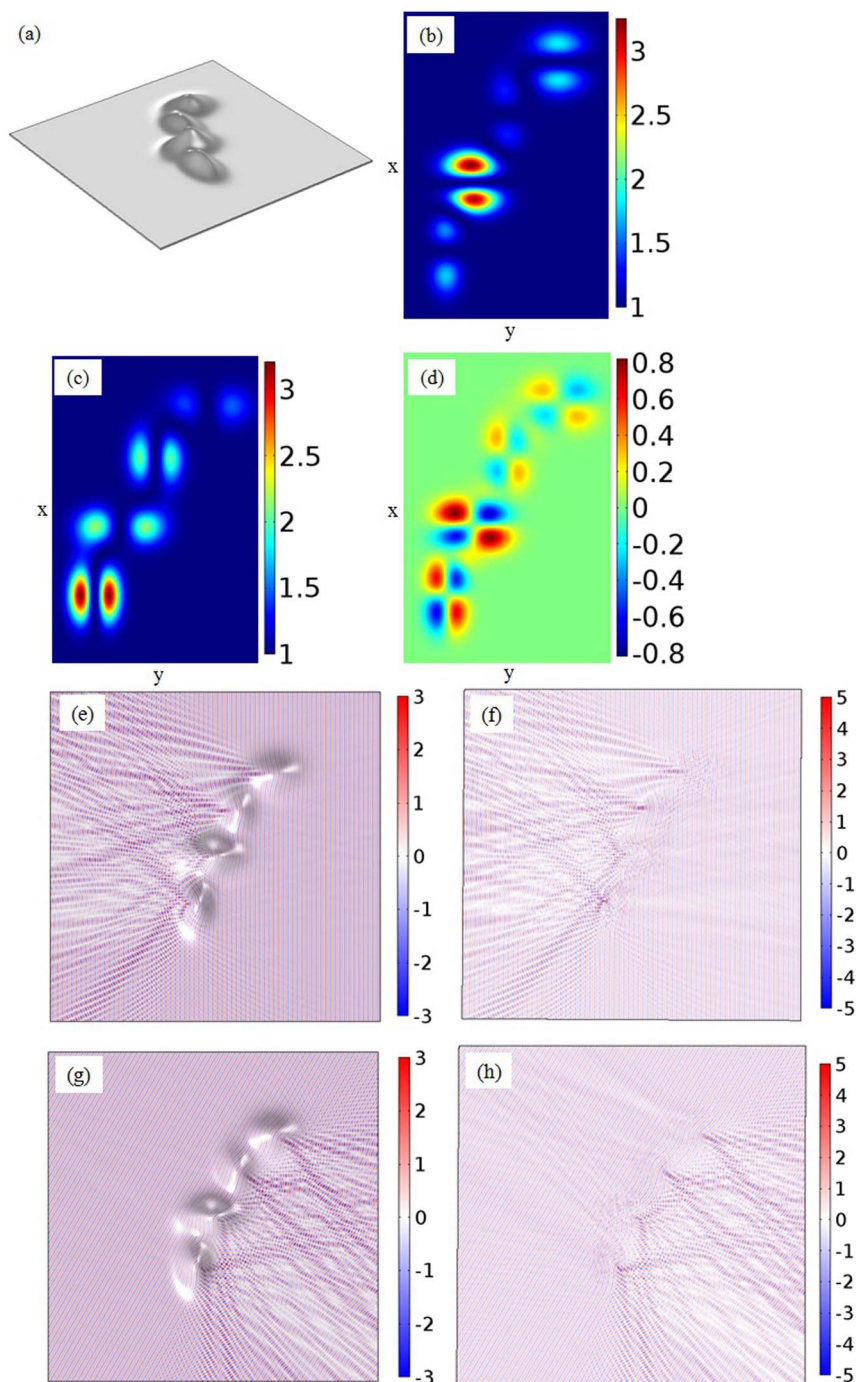
Figure 4 | Multiple deformations illusion device. The method of excitation for this simulation is identical to the one described for the singular surface deformation (a) Isometric view of S_2 (b) ε,μ_{xx}. (c) ε,μ_{yy}. (d) ε,μ_{xy}. Plane wave propagating (E_z) from right to left ($\theta_i = 0$), for curved isotropic medium (e) and flat anisotropic medium (f). Plane wave propagating (E_z) at $\theta_i = \dfrac{5\pi}{6}$ for a curved isotropic medium (g) and a flat anisotropic medium (h).

illusion device to reproduce the forward-SWS a quantitative study was also conducted. Two probe lines (Fig. 2), each $15\lambda_0$ in length are centered $15\lambda_0$ away from the origin of the deformation, and oriented in parallel to incident surface. In the first instance, θ is set to zero, and the amplitude of E_z along the red probe line is plotted (Fig. 3a). Here we note excellent agreement between the curved surface and the illusion device. Next we change the angle of incidence of the surface wave to $\dfrac{\pi}{4}$ and plot the amplitude of E_z along the blue probe line (Fig. 2). Once again, we note an excellent level of agreement between the curved surface and the illusion device (Fig. 3b). Taking these results, and those in Fig. 1, into account one can conclude that the

illusion device faithfully recreates the forward-SWS characteristics of its curved analogue.

Next, we consider how we might apply this proposed technique to a real-world scenario where a perturbation is not a simple, singular curve, namely a surface S_2, without axial or rotational symmetry. This surface is effectively a number of S_1 surfaces existing very close to one-another, but with no two sub-surfaces having the same height, origin or slope (along x or y). The net result of this juxtaposition of arbitrary, asymmetric, revolved Gaussian deformations is something akin to a group of rolling hills, and can be found in Fig. 4a. Once again, we note that the flat, metallic surface coated with proscribed material properties perfectly reproduces both the forward and back-
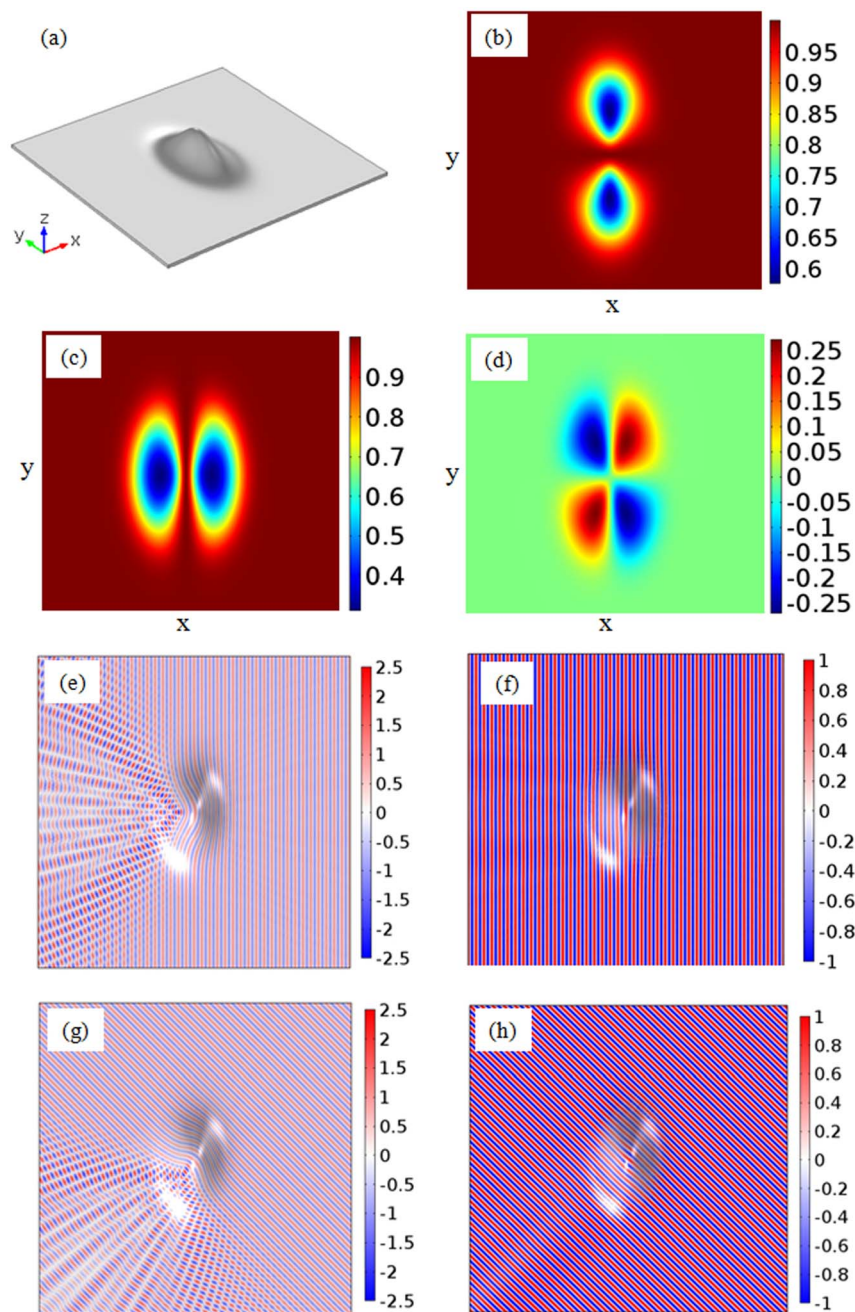
Figure 5 | Single deformation cloaking device. (a) Isometric view of S_1. (b) ε,μ_{xx}. (c) ε,μ_{yy}. (d) ε,μ_{xy}. Plane wave propagating (E_z) from right to left ($\theta_i = 0$), for curved isotropic medium (e) and curved, loaded, anisotropic medium (f). Plane wave propagating (E_z) at $\theta_i = \frac{\pi}{4}$ for curved isotropic medium (g) and curved, loaded, anisotropic medium (h).

ward-SWS characteristics of the original curved surface (Fig. 4e–h). It should be noted that the fact that primitive "sub-surfaces" can be used to build far more complex designs without sacrificing performance bodes well for future applications. In terms of applications, an electromagnetic illusion device would be useful if a designer needed to recreate the forward-SWS characteristics of a curved surface whilst simultaneously trying to minimize (flatten) the space that which this device occupied, as might occur in the design of a surface wave antenna.

Next, we derived the material parameters of a device that can cloak a rotationally asymmetric deformation from a surface wave. As one would imagine cloaking and illusion devices, for surface waves, rely on the same fundamental framing. We recall that for the illusion device we solved for the material parameters of a flat

surface that would render it electrically deformed. Now, however, for the case of the cloaking device we want to solve for the material parameters of a deformed surface that would render it electrically flat.

Starting from equation (1c) and going through a derivation similar to that of the illusion device, we arrive at

$$\tilde{\mu} = \frac{1}{1+(\nabla\sigma)^2}\begin{pmatrix} 1+\left(\frac{\partial\sigma}{\partial x}\right)^2 & \left(\frac{\partial\sigma}{\partial x}\right)\left(\frac{\partial\sigma}{\partial y}\right) \\ \left(\frac{\partial\sigma}{\partial x}\right)\left(\frac{\partial\sigma}{\partial y}\right) & 1+\left(\frac{\partial\sigma}{\partial y}\right)^2 \end{pmatrix} \quad (8)$$

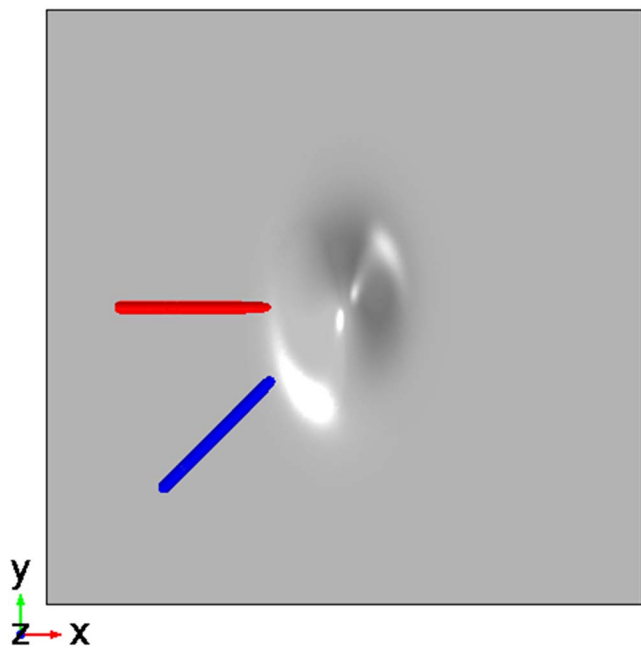whereas before, the surface under investigation is described as $z = \sigma(x,y)$.

Figure 6 | Probe line locations for cloaking device validation.

Figure 7 | Quantitative validation of proposed cloaking device. (a) $\theta_i = 0$ (b) $\theta_i = \dfrac{\pi}{4}$.

The test surface is once again an asymmetric Gaussian deformation (Fig. 5a) whose profile for the sake of continuity is identical to that of the one used in the illusion device example. The material parameters to cloak such a deformation, as defined by the proposed solution, appear in Fig. 5b–d. As expected, all of the required relative permittivity and permeability values are less than unity, which allow the phase fronts to traverse the deformation at a faster rate than their flat-space analogues, thereby giving rise to planar wave fronts in the forward-SWS region. The method of excitation and simulation for the cloak is identical to that of the illusion device, the results of which can be seen in Fig. 5e–h. Initially, a surface wave, is launched across the deformation at an angle of incidence of 0, for both the "unloaded" (Fig. 5e) and the "loaded" (Fig. 5f) case. True to form, the cloak completely renders the deformation electrically flat as is demonstrated by the total SWS (both forward and backward) in Fig. 5f. This process is repeated but for a different angle of incidence (Fig. 5g, h), and once again we observe a practically perfect cloaking performance (Animation 3).

The minor amplitude variations of E_z (Fig. 5h) that appear in the "shadow-region" are due to the underlying GO approximation employed in the proposed solution. Such an approximation places limitations on how fast the phase of a wave can change relative to the material parameters of the media in which the wave is propagating. The operating frequency is held constant through both of the aforementioned simulations, but the path at which the wave traverses now changes depending on the angle of incidence of the surface wave (owing to the rotationally asymmetric nature of the surface). Keeping this in mind, the minor shadowing displayed in Fig. 5h can be accounted for by the rate of change of the material parameters on the cloak exceeding the allowable limits set by GO. Keeping in line with the quantitative method used to validate the proposed illusion device's performance we do the same for the cloaking device (Fig. 6). Here the two probe lines, each $10\lambda_0$ in length, whose centers are $15\lambda_0$ away from the origin of the deformation, are oriented as is shown in Fig. 6. In the first instance, θ is set to zero, and the amplitude of E_z along the red probe line is plotted (Fig. 7a). Here we note that, as expected, due to the interference pattern created in the wake of the uncloaked surface deformation, the amplitude of E_z varies as it traverses down the probe-line (black curve in Fig. 7a). The cloaked surface deformation however, perfectly reproduces the characteris-
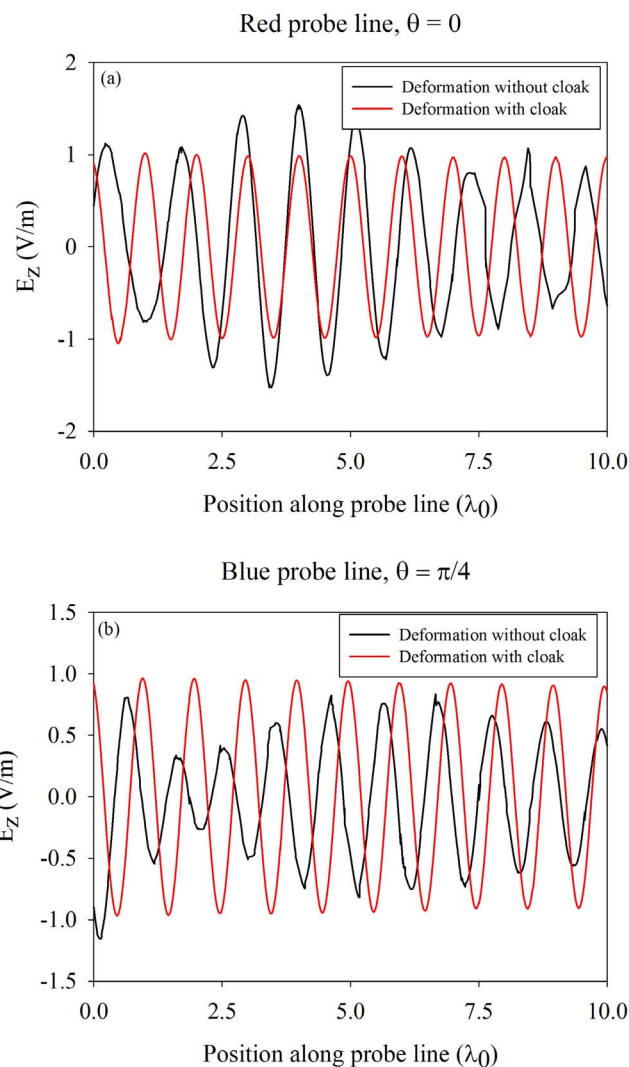
tics of a plane wave (red curve in Fig. 7a), as one would expect. Next, the angle of incidence of the surface wave is set to $\dfrac{\pi}{4}$ and the amplitude of E_z along the blue probe line is plotted (Fig. 6). Once again, we see the expected interference pattern created in the wake of the uncloaked deformation (black curve in Fig. 7b), while the cloaked deformation perfectly recreates the behavior of a plane-wave (red curve in Fig. 7b). Taking these results, and those in Fig. 5, into account one can conclude that the proposed cloaking device faithfully cloaks the surface deformation from surface waves.

In this Letter we have proposed a general method to engineer arbitrary illusion and cloaking devices for surface waves. For the case of illusion devices, it is achieved by utilising a thin sub-wavelength coating of an anisotropic material to perfectly recreate the total scattering characteristics of an arbitrary surface for all angles of incidence as was demonstrated in a full-wave electromagnetic solver (COMSOL 4.3b). For the cloaking device, a similar derivation to that of the illusion device is employed, and an asymmetric deformation coated with a anisotropic material, is shown to behave as if were a flat surface for all angles of incidence. The proposed illusion and cloaking devices, serve as proofs-of-concept for a highly generalized technique that can be adapted to other waves in fields such as thermodynamics and acoustics.

1. Leonhardt, U. Optical conformal mapping. *Science* **312**, 1777 (2006).
2. Leonhardt, U. & Philbin, T. G. General Relativity in electrical engineering. *New J. Phys.* **8**, 247 (2006).
3. Leonhardt, U. & Philbin, T. G. *Geometry and Light: The Science of Invisibility* (Dover Publications, New York, 2010).
4. Pendry, J. B., Schurig, D. & Smith, D. R. Controlling electromagnetic fields. *Science* **312**, 1780 (2006).
5. Farhat, M., Enoch, S., Guenneau, S. & Movchan, A. B. Broadband cylindrical acoustic cloak for linear surface waves in a fluid. *Phys. Rev. Lett.* **101**, 134501 (2008).
6. Guenneau, S., Amra, C. & Veynante, D. Transformation thermodynamic: cloaking and concentrating heat flux. *Opt. Express* **20**, 8207–8218 (2012).
7. Schurig, D. *et al.* Metamaterial electromagnetic cloak at microwave frequencies. *Science* **314**, 977 (2006).
8. Leonhardt, U. & Tyc, T. Broadband invisibility by non-Euclidean cloaking. *Science Express* **323**, 110 (2008).
9. Cai, W., Chettiar, U. K., Kildishev, A. V. & Shalaev, V. M. Optical cloaking with metamaterials. *Nature Photonics* **1**, 224–227 (2007).
10. Li, J. & Pendry, J. B. Hiding under the carpet: a new strategy for cloaking. *Phys. Rev. Lett.* **101**, 203901 (2008).
11. Lai, Y., Chen, H., Zhang, Z. & Chan, C. T. Complementary media invisibility cloak that cloaks objects at a distance outside of the cloaking shell. *Phys. Rev. Lett.* **102**, 093901 (2009).
12. Mitchell-Thomas, R. C., McManus, T. M., Quevedo-Teruel, O., Horsely, S. A. R. & Hao, Y. Perfect surface wave cloaks. *Phys. Rev. Lett.* **111**, 213901 (2013).
13. Chen, T. & Yu, S. R. Design of optical cloaks and illusion devices along a circumferential direction in curvilinear. *J. Appl. Phys.* **108**, 093106 (2010).
14. Ma, Q., Mei, Z. L., Zhu, S. K., Jin, T. Y. & Cui, T. J. Experiments on active cloaking and illusion for laplace equation. *Phys. Rev. Lett.* **111**, 173901 (2013).
15. Lai, Y. *et al.* Illusion optics: the optical transformation of an object into another object. *Phys. Rev. Lett.* **102**, 253902 (2009).
16. Zheng, H. H., Xiao, J. J., Lai, Y. & Chan, C. T. Exterior optical cloaking and illusions by using active sources: a boundary element perspective. *Phys. Rev. B* **81**, 195116 (2010).
17. Quarfoth, R. & Sievenpiper, D. Surface Wave Scattering Reduction Using Beam Shifters. *IEEE Antennas and Wireless Propagation Letters* **13**, 963–966 (2014).
18. Kim, S. & Sievenpiper, D. Theoretical Limitations for TM Surface Wave Attenuation by Lossy Coatings on Conductive Surfaces. *IEEE Transactions on Antennas and Propagation.* **62**, 475–480 (2014).
19. Kwon, D. H. & Emiroglu, C. D. Non-Orthogonal Grids in Two-Dimensional Transmission-Line Metamaterials. *IEEE Transactions on Antennas and Propagation* **60**, 4210–4218 (2012).
20. Zedler, M. & Eleftheriades, G. V. Anisotropic Transmission-Line Metamaterials for 2-D Transformation Optics Applications. *Proceedings of the IEEE* **99**, 1634–1645 (2011).
21. Patel, A. M. & Grbic, A. Transformation Electromagnetics Devices Based on Printed-Circuit Tensor Impedance Surfaces. *IEEE Transactions on Microwave Theory and Techniques* **62**, 1102–1111 (2014).
22. Gok, G. & Grbic, A. Tensor Transmission-Line Metamaterials. *IEEE Transactions on Antennas and Propagation* **58**, 1559–1566 (2010).
23. Werner, D. & Kwon, D. *Transformation Electromagnetics and Metamaterials* (Springer, London, 2013).
24. Walter, C. H. Surface-wave luneberg lens antennas. *IRE Trans. Antennas Propag.* **8**, 508 (1960).

Acknowledgments

Author contributions

S.A.R.H. and J.A.V.K. provided the physical derivation of the illusion and cloaking devices. T.M.M. implemented the derivation, simulated the candidate devices and produced the manuscript. Y.H. supervised the research.

Additional information